

# Bendable disordered metamaterials for broadband terahertz invisibility

DONG LIU,<sup>1</sup> YU-LIANG HONG,<sup>1</sup> REN-HAO FAN,<sup>1,4</sup> HAO JING,<sup>1</sup>  
RU-WEN PENG,<sup>1,5</sup> YUN LAI,<sup>1</sup> XIAN-RONG HUANG,<sup>2</sup> CHENG SUN,<sup>3</sup>  
AND MU WANG<sup>1,6</sup>

<sup>1</sup>National Laboratory of Solid State Microstructures, School of Physics, and Collaborative Innovation Center of Advanced Microstructures, Nanjing University, Nanjing 210093, China

<sup>2</sup>Advanced Photon Source, Argonne National Laboratory, Argonne, Illinois 60439, USA

<sup>3</sup>Department of Mechanical Engineering, Northwestern University, Evanston, Illinois 60208-3111, USA

<sup>4</sup>e-mail: rhfan@nju.edu.cn

<sup>5</sup>e-mail: rwpeng@nju.edu.cn

<sup>6</sup>e-mail: muwang@nju.edu.cn

**Abstract:** We experimentally demonstrate a bendable cloaking structure composed of obliquely stacked planar metallic shells that individually enclose the objects to be hidden. The ensemble of shells acts as a disordered oblique grating capable of bending along a curved structure and exhibits broadband invisibility from 0.2 to 1.0 THz. Hiding cloaked objects sized hundreds of microns could prevent the detection of certain powders that are sensitive to terahertz waves; such a cloaking structure can also be considered as a shape-changing passageway where the electromagnetic waves can pass through without changes at least in intensities and phases. Our approach provides a unique way to achieve broadband electromagnetic invisibility.

© 2019 Optical Society of America under the terms of the [OSA Open Access Publishing Agreement](#)

## 1. Introduction

Invisibility cloaks have been widely studied over the past few decades; the primary underlying principle is the prevention of the reflection and scattering of light by the cloaked object to render it imperceptible. Several approaches have been explored to realize this, such as transformation-based cloaks [1–5], carpet cloaks [6–8], plasmonic cloaks [9], transmission-line [10] or inductor–capacitor [11] networks, a non-Euclidian transformation [12], anomalous resonance methods [13], surface-wave transformation cloak [14], and unimodular transformation [15]. The majority of these cloaking mechanisms are only effective for a single specific frequency or within a very narrow bandwidth. Although carpet cloaks using non-resonant elements can realize broadband invisibility with low loss [6,16–18], and ray-optics and diffusive-light cloaks produced from glass or polymer can hide large objects in incoherent light in the visible-light region [19,20], these broadband invisibility cloaks require a large volume of space and are not bendable.

Meanwhile, bulk metals are known to be naturally opaque to light. Novel broadband transmission methods that have been proposed to obtain metals that are broadband invisible, include methods based on non-resonant excitations of spoof surface plasmons (SSPs) or surface plasmons (SPs) [21–25], the coupling of guided resonance modes [26], and the asymmetric transmission effect in metamaterials [27,28]. Oblique metal gratings have been demonstrated to become transparent to broadband terahertz (THz) waves under normal incidence; this transparency property is based on a non-resonance mechanism [24], but is still adversely affected by Wood’s anomalies, which are intrinsic diffraction properties of periodic structures, and which can significantly reduce the bandwidth of transparency. Fortunately, aperiodic metallic gratings are capable of weakening and even eliminating Wood’s anomalies, leading to an increase in the bandwidth of transparency [25]. Because the transparency is determined only by the surface of these metal structures, it is possible to hide the objects below the metallic

surface; this characteristic could possibly be exploited by devising a novel low-cost and simple method to fabricate invisibility cloaks to prevent objects from being detected by electromagnetic waves with a large bandwidth. However, metal structures that are known to be broadband transparent are not bendable. Flexible and conformable structures [29–34] with broadband invisibility, which cannot be detected by electromagnetic radiation over a wide range of frequencies and which can be bent into different shapes, are highly desirable for various practical applications.

In this study, we theoretically propose and experimentally demonstrate a bendable cloaking structure composed of obliquely stacked planar metallic shells which individually enclose the objects to be hidden. The ensemble of shells, which acts as a disordered oblique grating and is capable of bending along a curved structure, exhibits broadband invisibility from 0.2 to 1.0 THz. This transparency property is based on a non-resonance mechanism, which shows that the property of broadband invisibility is only determined by the relation between the tilt angle and duty cycle of the grating, regardless of the thickness of the grating. Moreover, when such a bendable metamaterial is bent along a curved structure, it still transmits THz waves, and the phase difference between the bendable metamaterial and free space can be suppressed by the average effect from different units, which leads to broadband invisibility.

## 2. Bendable disordered metamaterials for broadband terahertz invisibility

A bendable cloaking structure that is not bent (disordered oblique grating) is schematically shown in Fig. 1(a); a unit of this grating is the metal shell (with neglected metal thickness) with width  $a$ , thickness  $h$ , and tilt angle  $\phi$ , and the neighboring units are separated by a slit with a width  $p$ . The cloaked objects hidden inside the metallic shells can be composed of any material that would not undergo a chemical reaction with the metallic shells. A bendable cloaking structure formed by bending the disordered oblique grating along a curve is shown in Fig. 1(b). The radius of curvature is  $R$ . **Transverse-magnetic (TM) polarized electromagnetic waves** can efficiently be transmitted through the slits, regardless of the disordered structure; thus, any cloaked objects underneath the metallic shell would be undetectable to **TM polarized electromagnetic waves** and become invisible.

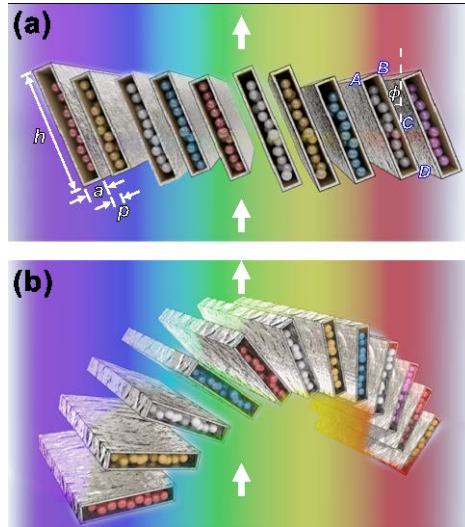


Fig. 1. Schematic representation of a cloaking structure: (a) an unbent bendable cloaking structure; a unit of this disordered grating is a metal shell with width  $a$ , thickness  $h$ , and tilt angle  $\phi$ , and neighboring units are separated by a slit with a width of  $p$ . The cloaked objects are hidden inside the metallic shells. (b) A bent cloaking structure with a radius of curvature  $R$ . **White arrows indicate the direction of electromagnetic waves at normal incidence.**

We experimentally show that an unbent bendable cloaking structure can act as an invisibility cloak in the THz range. As an example, we used strips coated with GaAs powder as the cloaked objects. Bulk GaAs (Tebo Technology Co., Ltd.) was ground to form GaAs powder; then, this powder was mixed with AB glue (Deli, 7148) and spread on the upper surface of a piece of 0.14-mm-thick paper, which was cut into several strips with random strip widths in the range of 3.5–4.5 mm. These strips were used to construct a disordered oblique GaAs-coated grating (cloaked objects) with random strip widths  $a$  (0.2–0.3 mm), random strip thicknesses  $h$  (3.5–4.5 mm), random slit widths  $p$  (0.10–0.18 mm), and a tilt angle  $\phi = 36^\circ (\pm 1^\circ)$ . Then, similar strips were covered with conductive silver paint (MECHANIC, MCN-DJ002). Upon drying, the paint formed a shell consisting of a metal film with a thickness of approximately 1.0–2.0  $\mu\text{m}$  around the strips. These strips with the thin metal film coating were then used to construct a disordered oblique grating (cloaking structure, as shown in Fig. 2(a)) with parameters similar to the disordered oblique GaAs-coated grating (cloaked objects).

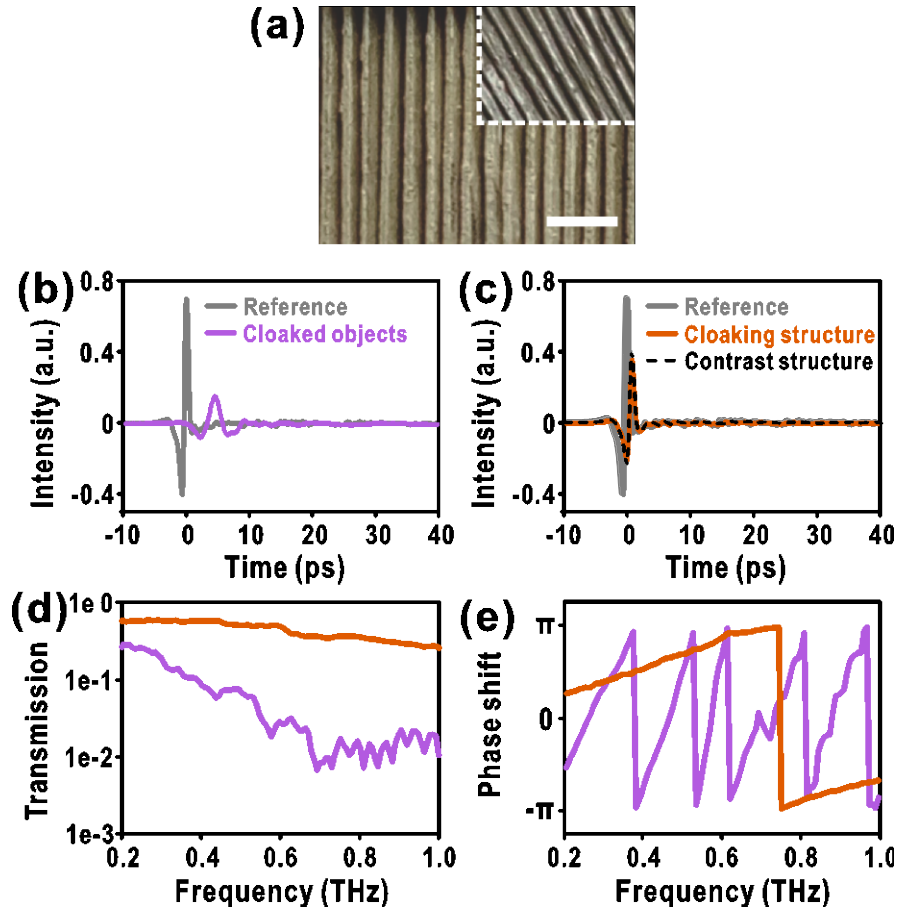


Fig. 2. (a) Optical images of the unbent cloaking structure; the insets show the respective cross sections, and the scale bar is 2 mm. (b) Measured time-domain spectra for the THz radiation transmitted through the cloaked objects; the reference spectrum is that of dry air. (c) Measured time-domain spectra for the THz radiation transmitted through the cloaking structure and the contrast structure; the reference spectrum is that of dry air. (d) Measured transmission spectra of the cloaked objects and cloaking structure. (e) Phase shifts for the cloaked objects and cloaking structure with respect to freely propagating waves.

Using a THz real-time spectrometer (EKSP/THz, Lithuania), we measured the time-domain signal  $E(t)$  of the THz pulse transmitted through the cloaked objects and cloaking structure, as shown in Figs. 2(b) and 2(c). The time-domain signal of the cloaked objects has a significant time delay compared to that of the air, whereas such a time delay is nearly absent from the time-domain signal of the cloaking structure. This indicates that the cloaking structure conceals information about the objects it covers. Clearly, the transmission spectrum of the cloaking structure is nearly flat, and the transmission intensity of the cloaking structure is much higher than that of the cloaked objects (by an order of magnitude ranging from nearly 0.4 to 1.0 THz), as shown in Fig. 2(d). The phase shifts of the transmitted waves with respect to waves that are freely propagating in air are shown in Fig. 2(e). The phase shift induced by the cloaked objects increases sharply with the frequency and contains small oscillations. However, no sharp phase changes or oscillations are observed on the transmission spectrum of the cloaking structure. This experimentally confirms that the disordered oblique gratings consisting of metal shells act as an invisible structure capable of allowing high and robust transmission of electromagnetic waves. We compare the cloaking structure with the paper covered with conductive silver paint while without the particles (contrast structure) as shown in Fig. 2(c), we can see similar time-domain signals of these two structures, so the information of particles is indeed being clocked.

We next discuss the underlying high and robust transmission mechanism of the proposed invisibility cloak. The simulation results for a periodic oblique grating and two disordered oblique gratings consisting of metal shells are shown in Fig. 3. These results were obtained by a finite-difference time-domain method [35] using a commercial software package (Lumerical FDTD Solution 8.0.1), and the metal can be regarded as a perfect electrical conductor. For a typical periodic oblique grating, a metal film with a thickness of  $2 \mu\text{m}$  is used to form the metal shells with width  $a = 0.25 \text{ mm}$ , thickness  $h = 4 \text{ mm}$ , slit width  $p = 0.14 \text{ mm}$ , and tilt angle  $\phi = 36^\circ$ , and it can be seen that excellent transmission is achieved within the broadband THz regime, with the exception of a sharp decrease at  $0.6 \text{ THz}$  originating from Wood's anomaly, as shown in Fig. 3(a). The uniform phase map of the electromagnetic waves shows that this structure hardly disturbs the electromagnetic waves, as shown in Fig. 3(b). To achieve broadband transparency for a typical periodic oblique grating under normal incidence, the tilt angle  $\phi$  of the oblique metal gratings should be optimized first. The optimal tilt angle  $\phi_f$  of the grating can be derived based on the force-balance condition [23]. When the light illuminates the oblique metal grating in Fig. 1(a), the incident electric field  $\mathbf{E}_m$  drives the movement of free electrons on the top surface  $AB$  and part of the slit wall  $BC$ , thus acting as a driving force on the electrons, thereby causing them to move on  $AB$  and  $BC$ . When the total forces exerted on  $AB$  and  $BC$  are balanced, the electrons can move smoothly around corner  $B$  without charge accumulation. Then, the charge waves formed on  $AB$  and  $BC$  may propagate continuously on the unilluminated wall  $CD$  to the bottom, resulting in strong light transmission through the slits. When the total force applied to the surface  $AB$  is equal to that applied to the illuminated slit wall  $BC$ , we can obtain the optimal tilt angle  $\phi_f$  as:  $\tan \phi_f (1 + \tan^2 \phi_f) / (1 + \tan \phi_f) = a / (a + p)$ , where  $\phi_f$  is only determined by the duty cycle  $a / (a + p)$ , and is independent of the strip thickness  $h$  [24]. Fortunately, the tolerance between tilt angle  $\phi$  and the duty cycle is sufficiently large to achieve high transmission [24], and thus, the duty cycle can vary within 53–75% in the above experiment with a fixed tilt angle  $\phi = 36^\circ$ . Because this high transmission is independent of the strip thickness  $h$ , electromagnetic waves can indeed be transmitted through the slits with random thicknesses  $h$  (3.5–4.5 mm), and the phase map is nearly flat, as shown in Figs. 3(d) and 3(e). Furthermore, because this high transmission also occurred within a duty cycle with a relatively wide range, electromagnetic waves can be transmitted through the slits with both random thicknesses  $h$  (3.6–4.4 mm) and random slit widths  $p$  (0.12–0.16 mm) with fixed width  $a = 0.25 \text{ mm}$ , and the wavefront of the transmission is relatively flat as shown in Figs. 3(g) and 3(h). Only part of the disordered structures is shown in Figs. 3(e) and 3(h), 30 different strips

are used in the calculation. On the basis of these results, it could be deduced that the high transmission is robust and independent of the non-uniform structural parameters.

We additionally calculated the dispersion maps for these three structures to show both broadband and broad-angle high transmission. The dispersions were calculated for the oblique gratings with a periodic structure (Fig. 3(c)), random thicknesses (Fig. 3(f)), and both random thicknesses and metallic shell widths (Fig. 3(i)), respectively. The areas of high transmission occur within the dashed white lines in the low-frequency region of these dispersion maps, indicating both broadband and broad-angle high transmission; this high transmission is robust against disordered structures. Based on the results presented thus far, it could be concluded that the above metamaterial composed of oblique metal gratings can achieve high transmission that is robust against disordered structures. This suggested that it would be possible to utilize this robustness to achieve invisibility. The cloaked objects (with a width less than the wavelength) intended to be hidden can be composed of any material that is chemically inert with respect to the metallic shells. The cloaking is based on the following principle: structures exposed to electromagnetic waves would transmit the waves through the obliquely stacked planar metallic shells and the waves would remain unaffected by the cloaked objects inside the metallic shells, as though these objects did not even exist.

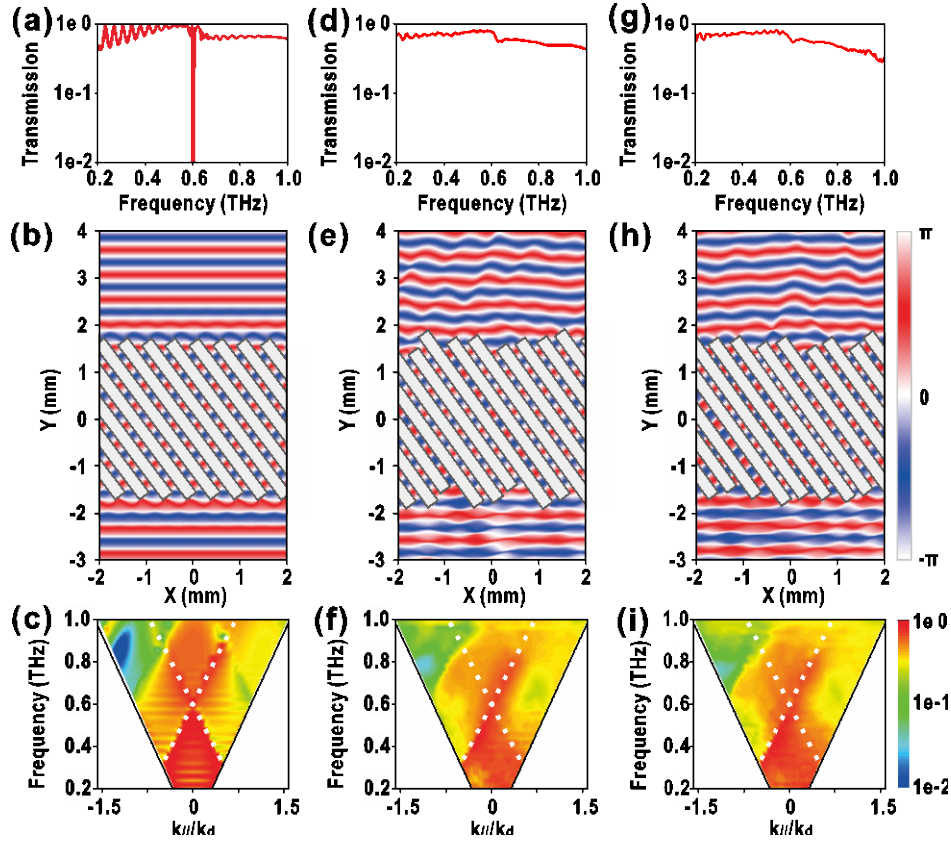


Fig. 3. (a) Calculated transmission spectrum, (b) phase map at 0.57 THz, and (c) dispersion for a periodic oblique grating consisting of uniform metal shells. (d) Calculated transmission spectrum, (e) phase map at 0.57 THz, and (f) dispersion for a disordered oblique grating consisting of metal shells with non-uniform thickness  $h$ . (g) Calculated transmission spectrum, (h) phase map at 0.57 THz, and (i) dispersion for a disordered oblique grating consisting of metal shells with non-uniform thickness  $h$  and non-uniform width  $a$ . The incident electromagnetic waves illuminate the bottom surface and are transmitted to the top.

Most importantly, we can tune the tilt angle  $\phi$  to observe its influence on the invisibility. The calculated transmission spectra of the periodic oblique gratings consisting of metal shells with different tilt angles  $\phi$  are shown in Fig. 4(a), and it can be seen that broadband high transmission occurs within a broad range of tilt angles, particularly from  $20^\circ$  to  $50^\circ$ . The phase shift with respect to freely propagating waves after passing through the oblique gratings for different tilt angles  $\phi$  is shown in Fig. 4(b); the phase shift for the incident wave changes gradually when  $\phi$  increases (or decreases) because the equivalent optical path is gradually changed. Thus, broadband high transmission can also be achieved for a curved cloaking structure (curved disordered oblique grating), and the phase shift of this curved cloaking structure could be suppressed, because the phase shift of the entire structure is the average effect of the units with different tilt angles.

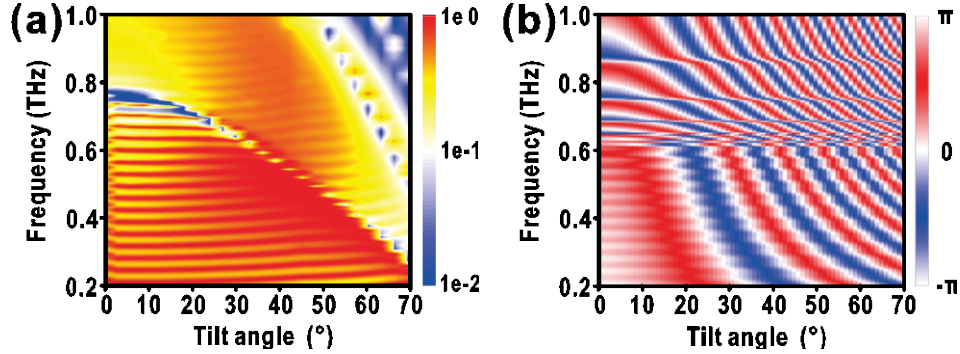


Fig. 4. (a) Calculated transmission spectra of oblique gratings consisting of metal shells with different tilt angles  $\phi$ . (b) Phase shift with respect to freely propagating waves after passing through the oblique gratings for different tilt angles  $\phi$ .  $a = 0.25$  mm,  $h = 4$  mm,  $p = 0.14$  mm.

The disordered oblique grating consisting of metal shells forms a bendable cloaking structure; a curved cloaking structure is obtained by bending the cloaking sample shown in Fig. 2(a). A cross-sectional image of the curved cloaking structure is shown in Fig. 5(a); the radius of curvature for this sample is approximately 2.7 cm. The transmission spectra were measured for both the curved cloaking structure (curved disordered oblique grating consisting of metal shells) and the curved cloaked objects (curved disordered oblique GaAs-coated grating without metal shells). The results showed that the transmission of the curved cloaking structure is nearly flat, and it is much higher than that of the cloaked objects in the range 0.2–1.0 THz, as shown in Fig. 5(b). The phase shift of the curved cloaked objects increases sharply at low frequencies and exhibits wide fluctuations at high frequencies, as shown in Fig. 5(c). In contrast, the phase shift of the curved cloaking structure is largely eliminated by the average effect of each unit with different tilt angles and only changes slightly with the frequency, as shown in Fig. 5(c). A model with a gradual phase change can be used to understand the suppression of the phase shift in the curved cloaking structure. For the curved cloaking structure, the phase change for each unit is different, and  $\phi$  changes gradually as the position of the structure varies in space. Therefore, with respect to freely propagating waves, the phase shift changes gradually after passing through the curved cloaking structure. The phase shift of the entire structure is an average effect resulting from the different tilt angles of the units. Thus, we carefully selected the radius of curvature at which the detected phase shift of the curved cloaking structure becomes nearly constant and tends to zero from 0.2 to 1.0 THz in the experiment. This is an intriguing result suggesting that a bendable curved cloaking structure could also be invisible (the ideal situation) to achieve high and robust transmission with relatively small phase shifts. We also assessed this curved cloaking structure by recording the transmission spectra and measuring the phase difference at different incident angles, compared to that of normal incidence as shown in Figs. 5(d) and 5(e), respectively. These results show that the curved cloaking structure can, at minimum, function for incident angles ranging from  $-10^\circ$  to  $30^\circ$  (the

positive incident direction is defined to be identical to  $\phi$ ); within this range, the broadband high transmission is maintained and the phase changes slightly with the frequency. The applicable range of incident angles are  $-10^\circ$  to  $30^\circ$ , which is asymmetric because the structure as shown in Fig. 5(a) is asymmetric.

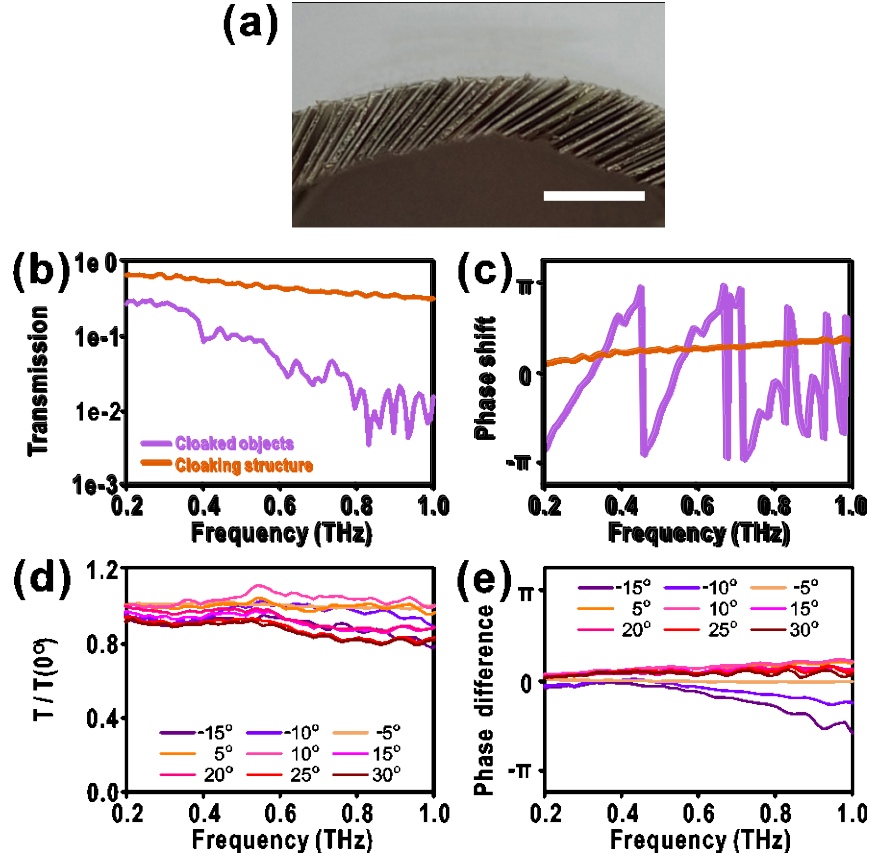


Fig. 5. (a) Cross-sectional image of the curved cloaking structure; the scale bar is 4 mm. (b) Measured transmission spectra for the curved cloaked objects and curved cloaking structure for normal incidence. (c) Phase shifts for the curved cloaked objects and curved cloaking structure with respect to freely propagating waves at normal incidence. (d) Measured transmission spectra and (e) phase difference for the curved cloaking structure for a case of oblique incidence compared to one of normal incidence.

It is worthwhile to emphasize the advantages and space for improvement for this bendable cloaking structure holds for practical applications. First, the structure retains its broadband invisibility when it is bent. Second, the transmission is robust against the disordered structure. Third, these cloaks are easy to fabricate by simply painting or spraying metallic thin films onto the target objects to be cloaked and arranging them as similar oblique gratings. Fourth, this cloaking is polarization-sensitive in present 1D case, but in principle, such type of cloaking can become polarization-insensitive in 2D or higher-dimensional structures. Fifth, the transmission in the experiment can be higher by using thicker metallic films or materials with better conductivity, e.g. coating thick metal films. Sixth, the sizes of the cloaked objects here are smaller than the metal shell width  $a$  and thickness  $h$ , compared to other cloaks which have one concealed volume, each metal shell in our structure can be used to hide objects, so the total volume for the cloaked objects to the volume of the sample is close to  $a / (a + p)$ .

### 3. Conclusions

Here, we demonstrated a bendable cloaking structure composed of obliquely stacked planar metallic shells that individually enclose the objects to be hidden. The ensemble of shells acts as a disordered oblique grating that can be bent to form a curved structure; this bendable cloaking structure exhibits broadband invisibility from 0.2 to 1.0 THz, and the curved cloaking structure is functionally effective for incident angles ranging from  $-10^\circ$  to  $30^\circ$ . A wide range of practical applications exists that would require hiding cloaked objects with sizes of the order of hundreds of microns, **which are smaller than the sizes of the metal shells**. These applications include preventing certain powders that are sensitive to THz waves from being detected, and providing a passageway to pass through THz waves without any interference by these waves themselves, **such as camouflaging and anti-detection**. In principle, similar cloaking effects can be achieved for a broad bandwidth of frequencies ranging from infrared to radio waves. Moreover, once extended to radio waves, these types of invisible structures could prevent small flying robots from being detected by radar.

### Funding

This work was supported by the Ministry of Science and Technology of China (2017YFA0303702), and the National Natural Science Foundation of China (11634005, 11974177, 11604143, 61975078, 11674155). And X.R.H. was supported US Department of Energy, Office of Science, Office of Basic Energy Sciences (DE-AC02-06CH11357).

### Disclosures

The authors declare no conflicts of interest.

### References

1. U. Leonhardt, "Optical conformal mapping," *Science* **312**, 1777–1780 (2006).
2. J. B. Pendry, D. Schurig, and D. R. Smith, "Controlling electromagnetic fields," *Science* **312**, 1780–1782 (2006).
3. H. Y. Chen, C. T. Chan, and P. Sheng, "Transformation optics and metamaterials," *Nature Mater.* **9**, 387–396 (2010).
4. C. Qian, R. Li, Y. Jiang, B. Zheng, H. Wang, Z. Xu, and H. Chen, "Transient response of a signal through a dispersive invisibility cloak," *Opt. Lett.* **41**, 4911–4914 (2016).
5. F. Liu, S. A. R. Horsley, and J. Li, "Invisibility cloaking using pseudomagnetic field for photon," *Phys. Rev. B* **95**, 075157 (2017).
6. J. Li, and J. B. Pendry, "Hiding under the carpet: a new strategy for cloaking," *Phys. Rev. Lett.* **101**, 203901 (2008).
7. X. Ni, Z. J. Wong, M. Mrejen, Y. Wang, and X. Zhang, "An ultrathin invisibility skin cloak for visible light," *Science* **349**, 1310–1314 (2015).
8. Y. Yang, L. Jing, B. Zheng, R. Hao, W. Yin, E. Li, C. M. Soukoulis, and H. Chen, "Full-polarization 3D metasurface cloak with preserved amplitude and phase," *Adv. Mater.* **28**, 6866–6871 (2016).
9. A. Alù, and N. Engheta, "Achieving transparency with plasmonic and metamaterial coatings," *Phys. Rev. E* **72**, 016623 (2005).
10. P. Alitalo, O. Luukkonen, L. Jylhä, J. Venermo, and S. A. Tretyakov, "Transmission-line networks cloaking objects from electromagnetic fields," *IEEE Trans. Antennas Propag.* **56**, 416–424 (2008).
11. C. Li, X. Liu, and F. Li, "Experimental observation of invisibility to a broadband electromagnetic pulse by a cloak using transformation media based on inductor-capacitor networks," *Phys. Rev. B* **81**, 115133 (2010).
12. U. Leonhardt, and T. Tyc, "Broadband invisibility by non-Euclidean cloaking," *Science* **323**, 110–112 (2009).
13. Y. Lai, H. Chen, Z. Q. Zhang, and C. T. Chan, "Complementary media invisibility cloak that cloaks objects at a distance outside the cloaking shell," *Phys. Rev. Lett.* **102**, 093901 (2009).
14. S. Xu, H. Xu, H. Gao, Y. Jiang, F. Yu, J. D. Joannopoulos, M. Soljačić, H. Chen, H. Sun, and B. Zhang, "Broadband surface-wave transformation cloak," *Proc. Natl. Acad. Sci. U. S. A.* **112**, 7635–7638 (2015).
15. B. Orzabayev, M. Beruete, A. Martínez, and C. García-Meca, "Diffusive-light invisibility cloak for transient illumination," *Phys. Rev. A* **94**, 063850 (2016).
16. R. Liu, C. Ji, J. J. Mock, J. Y. Chin, T. J. Cui, and D. R. Smith, "Broadband ground-plane cloak," *Science* **323**, 366–369 (2009).
17. F. Zhou, Y. Bao, W. Cao, C. T. Stuart, J. Gu, W. Zhang, and C. Sun, "Hiding a realistic object using a broadband terahertz invisibility cloak," *Sci. Rep.* **1**, 78 (2011).

18. D. Liang, J. Gu, J. Han, Y. Yang, S. Zhang, and W. Zhang, "Robust large dimension terahertz cloaking," *Adv. Mater.* **24**, 916–921 (2012).
19. H. Chen, B. Zheng, L. Shen, H. Wang, X. Zhang, N. I. Zheludev, and B. Zhang, "Ray-optics cloaking devices for large objects in incoherent natural light," *Nat. Commun.* **4**, 2652 (2013).
20. R. Schittny, M. Kadic, T. Bückmann, and M. Wegener, "Invisibility cloaking in a diffusive light scattering medium," *Science* **345**, 427–429 (2014).
21. X. R. Huang, R. W. Peng, and R. H. Fan, "Making metals transparent for white light by spoof surface plasmons," *Phys. Rev. Lett.* **105**, 243901 (2010).
22. A. Alù, G. D'Aguzzo, N. Mattiucci, and M. J. Bloemer, "Plasmonic Brewster angle: broadband extraordinary transmission through optical gratings," *Phys. Rev. Lett.* **106**, 123902 (2011).
23. R. H. Fan, R. W. Peng, X. R. Huang, J. Li, Y. Liu, Q. Hu, M. Wang, and X. Zhang, "Transparent metals for ultrabroadband electromagnetic waves," *Adv. Mater.* **24**, 1980–1986 (2012).
24. R. H. Fan, J. Li, R. W. Peng, X. R. Huang, D. X. Qi, D. H. Xu, X. P. Ren, and M. Wang, "Oblique metal gratings transparent for broadband terahertz waves," *Appl. Phys. Lett.* **102**, 171904 (2013).
25. X. P. Ren, R. H. Fan, R. W. Peng, X. R. Huang, D. H. Xu, Y. Zhou, and M. Wang, "Nonperiodic metallic gratings transparent for broadband terahertz waves," *Phys. Rev. B* **91**, 045111 (2015).
26. Z. Wei, Y. Cao, Y. Fan, X. Yu, and H. Li, "Broadband transparency achieved with the stacked metallic multilayers perforated with coaxial annular apertures," *Opt. Express* **19**, 21425–21431 (2011).
27. N. K. Grady, J. E. Heyes, D. R. Chowdhury, Y. Zeng, M. T. Reiten, A. K. Azad, A. J. Taylor, D. A. R. Dalvit, and H. -T. Chen, "Terahertz metamaterials for linear polarization conversion and anomalous refraction," *Science* **340**, 1304–1307 (2013).
28. J. H. Shi, H. F. Ma, C. Y. Guan, Z. P. Wang, and T. J. Cui, "Broadband chirality and asymmetric transmission in ultrathin 90°-twisted Babinet-inverted metasurfaces," *Phys. Rev. B* **89**, 165128 (2014).
29. M. Choi, S. H. Lee, Y. Kim, S. B. Kang, J. Shin, M. H. Kwak, K. -Y. Kang, Y. -H. Lee, N. Park, and B. Min, "A terahertz metamaterial with unnaturally high refractive index," *Nature* **470**, 369–373 (2011).
30. D. Chanda, K. Shigeta, S. Gupta, T. Cain, A. Carlson, A. Mihi, A. J. Baca, G. R. Bogart, P. Braun, and J. A. Rogers, "Large-area flexible 3D optical negative index metamaterial formed by nanotransfer printing," *Nature Nanotech.* **6**, 402–407 (2011).
31. X. Xu, B. Peng, D. Li, J. Zhang, L. M. Wong, Q. Zhang, S. Wang, and Q. Xiong, "Flexible visible-infrared metamaterials and their applications in highly sensitive chemical and biological sensing," *Nano Lett.* **11**, 3232–3238 (2011).
32. K. Iwaszczuk, A. C. Strikwerda, K. Fan, X. Zhang, R. D. Averitt, and P. U. Jepsen, "Flexible metamaterial absorbers for stealth applications at terahertz frequencies," *Opt. Express* **20**, 635–643 (2012).
33. A. P. Slobozhanyuk, M. Lapine, D. A. Powell, I. V. Shadrivov, Y. S. Kivshar, R. C. McPhedran, and P. A. Belov, "Flexible helices for nonlinear metamaterials," *Adv. Mater.* **25**, 3409–3412 (2013).
34. L. Cong, N. Xu, J. Gu, R. Singh, J. Han, and W. Zhang, "Highly flexible broadband terahertz metamaterial quarter-wave plate," *Laser Photonics Rev.* **4**, 626–632 (2014).
35. A. Taflove, and S. C. Hagness, *Computational Electrodynamics: The Finite-Difference Time-Domain Method* (Artech House, 2005).